Spectroscopic studies on the interaction of cationic surfactants with bovine serum albumin

ARTICLE · JANUARY 2009

CITATIONS
5

READS
21

6 AUTHORS, INCLUDING:

Nuzhat Gull
Government College for Women, Srinagar
14 PUBLICATIONS **216** CITATIONS
SEE PROFILE

Shirish Chodankar
Paul Scherrer Institut
25 PUBLICATIONS **245** CITATIONS
SEE PROFILE

Priyankar Sen
VIT University
19 PUBLICATIONS **420** CITATIONS
SEE PROFILE

Rizwan Hasan Khan
Aligarh Muslim University
228 PUBLICATIONS **3,191** CITATIONS
SEE PROFILE

Colloids and Surfaces B: Biointerfaces 69 (2009) 122–128

Contents lists available at ScienceDirect

Colloids and Surfaces B: Biointerfaces

journal homepage: www.elsevier.com/locate/colsurfb

Spectroscopic studies on the interaction of cationic surfactants with bovine serum albumin

Nuzhat Gull[a], Shirish Chodankar[b], V.K. Aswal[b], Priyankar Sen[c], Rizwan Hasan Khan[c], Kabir-ud-Din[a,*]

[a] Department of Chemistry, Aligarh Muslim University, Aligarh 202002, India
[b] Solid State Physics Division, Bhabha Atomic Research Centre, Mumbai 400085, India
[c] Interdisciplinary Biotechnology Unit, Aligarh Muslim University, Aligarh 202002, India

ARTICLE INFO

Article history:
Received 5 July 2008
Received in revised form
16 November 2008
Accepted 18 November 2008
Available online 25 November 2008

Keywords:
Serum albumin
SANS
Circular dichroism
Fluorescence spectroscopy

ABSTRACT

The interaction of the cationic surfactant cetyltrimethylammonium bromide (CTAB) with bovine serum albumin (BSA), a globular protein, has been studied by small-angle neutron scattering (SANS), fluorescence and circular dichroism (CD). SANS measurements show that at low [CTAB] the protein shows a native-like behavior. On the other hand, at high [CTAB], surfactant molecules result in the formation of a fractal structure representing a 'necklace model' of micelle-like clusters randomly distributed along the polypeptide chain. The overall size of the complex increases and the fractal dimension decreases on increasing the surfactant concentration. The size of the micelle-like clusters does not show any considerable change while the number of such clusters and their aggregation number increases with increasing [CTAB]. Some extrapolatory experiments were performed with tetradecyltrimethylammonium bromide (TTAB) and the surfactant was found to behave similarly leading to an increase in the size of protein along the semi-major axis at low concentrations and formation of a fractal structure at high concentrations. The fluorescence studies undertaken were found to be consistent with the SANS measurements. Native-like behavior of the protein mixed with low concentration of the surfactant was also concluded from the circular dichroism (CD) spectra where the spectra in presence of high [CTAB] could not be monitored because of high dynode voltage.

1. Introduction

The functions of a protein, considered to be the most abundant and versatile macromolecule, is directly dependent on its three dimensional structure. The protein–surfactant interactions have been a subject of extensive research [1,2] ever since the surfactants were found to be the denaturants of water soluble proteins [3]. Investigation of assembly, large scale conformational changes or folding/unfolding of the biological macromolecules are part of the broader search for organizing principles on the mesoscope scale. The understanding of protein folding/unfolding has not only provided an intellectual challenge but also has an immense potential for application. The solution of folding problem seems to be an important step in protein engineering and in understanding some diseases (amyloidoses) associated with misfolding of proteins and formation of amyloid fibrils [4].

Although the structure of many proteins is known at the level of atomic resolution, we do not have a clear concept of the physical principles of organization of these structures and the forces stabilizing them in space. Studying the process of denaturation of the native protein is an important approach to this problem. The denaturation of proteins may be done by denaturing agents such as urea, guanidine hydrochloride or ionic surfactants. The denaturation by the surfactants involves binding of the surfactant ions to sites on protein molecules while that by urea or guanidine HCl primarily depends on the effect of these compounds on water structure.

Due to the hydrophobic and hydrophilic properties of the amino acids, a protein exhibits dualism that makes small amphiphilic molecules interact with proteins. The amphiphilic molecules chosen to study the protein–surfactant complexes, in general, are the ionic surfactants in view of their application in the area of membrane studies [5,6]. Usually, surfactant binding with proteins depends on surfactant features. The formation of complexes between anionic surfactants and proteins in aqueous solutions have been well established [7–11]. Cationic surfactants have been found to interact with the proteins to a lesser extent compared to anionics mainly as a consequence of smaller relevance of electrostatic interactions at the pH's of interest [12]. However, the binding isotherms of both these type of surfactants have been found to be similar [13,14]. The conformational changes induced in the protein, when the surfactant binds to it, result in changes of polarity and the stability of the protein [7,8,14,15]. The interaction of surfactants with

* Corresponding author. Fax: +91 571 2708336.
E-mail address: kabir7@rediffmail.com (Kabir-ud-Din).

0927-7765/$ – see front matter © 2008 Elsevier B.V. All rights reserved.
doi:10.1016/j.colsurfb.2008.11.009

proteins is of importance in a wide variety of industrial, biological, pharmaceutical and cosmetic systems [16]. The mechanism of unfolding of proteins on addition of the surfactant has been studied by several techniques such as circular dichroism (CD) [17,18], nuclear magnetic resonance (NMR) [19], microcalorimetry [20], light scattering [21] and small-angle scattering [22–27]. Among the various proposed models of the protein–surfactant complexes such as rod-like, flexible helix model and the necklace model, the necklace model is the most accepted for the understanding of the interaction of these two components in their complex formation [28].

Small-angle neutron scattering (SANS) is an important tool in studies of biological macromolecules that allows to study native particles in nearly physiological solutions and to analyze structural changes in response to variations in external conditions. SANS has been used to evaluate the protein–surfactant complex as fractal structure based on the necklace model that comprise micelle-like clusters randomly distributed along the polypeptide chain of the unfolded protein [22]. This technique has been quite useful to yield detailed information, such as fractal dimension of the protein–surfactant complex characterizing the distribution of micelle-like clusters bound to the protein, the extent of the complex and the average size of the micelle-like clusters in the complex.

This paper details the interaction of a commonly used cationic surfactant cetyltrimethylammonium bromide (CTAB) with the physiologically vital bovine serum albumin (BSA) as studied by SANS, fluorescence and circular dichroism. Some extrapolatory measurements were also performed with tetradecyltrimethylammonium bromide (TTAB). The serum albumins consist of a globular protein synthesized by the liver in mammals corresponding to the most abundant protein in serum, accounting for 60% of the total globular protein in plasma corresponding to a concentration of 42 g/l and provide about 80% of the osmotic pressure of the blood [29–32]. Albumins have been used as model proteins for many diverse biophysical, biochemical and physico-chemical studies [33]. These proteins have the interesting properties of binding to a variety of hydrophobic ligands such as fatty acids, lysolecithin, bilirubin, warfarin, tryptophan, steroids, anesthetics and several dyes [34–37]. They play an important role in the transport and deposition of a variety of endogenous and exogenous substances in the blood [38] due to the existence of limited number of binding regions of very different specificity [39]. Serum albumins are also used in peritoneal dialysis in combating the harmful effect of antibiotics and as a scavenger of toxic substances and free radicals [40]. Albumin is an important constituent of tissue culture media [41]. It serves as a medium to support growth of microorganisms, e.g., bacteria, fungi and yeast [42].

2. Materials and methods

2.1. Materials

Bovine serum albumin (BSA) (Sigma, USA), cetyltrimethylammonium bromide (CTAB, Sigma), tetradecyltrimethylammonium bromide (TTAB, Sigma), 1-anilino-8-naphthalene sulfonic acid (ANS, Sigma) were used as received. Samples for SANS experiments were prepared by dissolving a known amount of BSA and the surfactants in a phosphate buffer solution (pH 7) of D_2O. The use of D_2O as solvent instead of H_2O provides better contrast for hydrogenous components in neutron experiments. Stock solutions of BSA (6.5 μM), CTAB and TTAB, prepared in a phosphate buffer (pH 7) using double distilled water, were utilized to prepare the samples of desired concentrations for fluorescence studies.

2.2. SANS measurements

Small-angle neutron scattering experiments were performed on the SANS instrument at Dhruva reactor, Bhabha Atomic Research Centre, Mumbai [43]. The mean wavelength of the incident neutron beam was 5.2 Å with a wavelength resolution of approximately 15%. The data were collected in the wave-vector transfer magnitude Q range of 0.018–0.35 $Å^{-1}$. The measurements were made for 1 wt% BSA in presence of varying concentrations of the surfactants. The measured SANS data were collected and normalized to a cross-sectional unit using standard procedures [44].

2.3. Data analysis

In small-angle neutron scattering (SANS), coherent differential scattering cross-section per unit volume $d\Sigma/d\Omega$ as a function of Q is measured. For a system of monodisperse interacting protein molecules, $d\Sigma/d\Omega(Q)$ can be expressed as [45]

$$\frac{d\Sigma}{d\Omega}(Q) = N_p V_p^2(\rho_p - \rho_s)^2\{\langle F^2(Q)\rangle + \langle F(Q)\rangle^2[S_p(Q) - 1]\} + B \quad (1)$$

where N_p is the number density of the protein, ρ_p and ρ_s is the scattering length density of the protein and the solvent and V_p is the volume of the protein molecule. $F(Q)$ is the single particle form factor and $S_p(Q)$ is the interparticle structure factor. B is a constant term that represents the incoherent scattering background, which is mainly due to hydrogen in the sample. The single particle form factor has been calculated by treating the protein macromolecules as a prolate ellipsoid. For such an ellipsoidal particle

$$\langle F^2(Q)\rangle = \int_0^1 [F(Q,\mu)^2\, d\mu] \quad (2)$$

$$\langle F(Q)\rangle^2 = \left\{\int_0^1 [F(Q,\mu)]\, d\mu\right\}^2 \quad (3)$$

$$F(Q,\mu) = \frac{3(\sin x - x\cos x)}{x^3} \quad (4)$$

$$x = Q[a^2\mu^2 + b^2(1-\mu^2)]^{1/2} \quad (5)$$

where a and b are, respectively, the semi-major and semi-minor axes of the ellipsoidal protein macromolecules and μ is the cosine of the angle between the directions of a and the wave-vector transfer Q.

In general, charged colloidal systems such as protein solutions show a correlation peak in the SANS distribution. The peak arises because of the interparticle structure factor $S_p(Q)$ and indicates the presence of electrostatic interaction between the colloids. In the case of low concentration of protein solution, $S_p(Q)$ can be approximated to unity as the interparticle interactions are minimized.

The unfolding of proteins has been modeled using the necklace model of protein–surfactant complexes that assumes micelle-like clusters of surfactant randomly distributed along the unfolded polypeptide chain. The cross-section for such a system can be expressed as [8,11]

$$\frac{d\Sigma}{d\Omega}(Q) = \frac{N_1^2}{N_p N}(b_m - V_m\rho_s)^2 P(Q) S_f(Q) + B \quad (6)$$

where N_1 is the number density of the total surfactant molecules in solution, V_m the volume of the micelle and N the number of such micelles attached to a polypeptide chain, b_m represents the scattering length of the surfactant molecule. $P(Q)$ denotes the normalized interparticle structure factor ($\langle F^2(Q)\rangle$) of a single micelle-like

cluster, which, for a spherical particle of radius R is given by [2]

$$P(Q) = \left[\frac{3\{\sin(QR) - QR\cos(QR)\}}{(QR)^3}\right]^2 \quad (7)$$

$S_f(Q)$ has been calculated using fractal structure for the necklace model of protein–surfactant complex. The arrangement of micelle-like clusters is assumed as fractal packing of spheres. In this case, $S_f(Q)$ is given as [46]

$$S_f(Q) = 1 + \frac{1}{(QR)^D}\frac{D\Gamma(D-1)}{[1+(Q\xi)^{-2}]^{[(D-1)/2)]}} \times \sin[(D-1)\tan^{-1}(Q\xi)]$$

where D is the fractal dimension of the micellar distribution in space and ξ the correlation length that is a measure of the extent of unfolding of the polypeptide chain.

The dimensions of the protein macromolecule at low surfactant concentrations have been determined from the analysis. The semi-major axis (a) and the semi-minor axis ($b = c$) are the parameters in analyzing the SANS data. At higher surfactant concentrations the fractal dimension (D), correlation length (ξ), number of micelles (N) and radius of micelles (R) are the fitted parameters to characterize the unfolding of protein. The aggregation number of the micelle-like clusters in the complex is calculated by $n = N_1/(N_pN)$. Throughout the data analysis, corrections were made for instrumental smearing. The parameters in the analysis were optimized by means of a non-linear least-square fitting program and the errors on the parameters were calculated by the standard method [47].

2.4. Fluorescence measurements

Fluorescence measurements were performed on Hitachi spectrofluorimeter (model 2500) equipped with a PC. The fluorescence spectra were collected at 25 °C with a 1 cm path length cell. The excitation and emission slits were set at 5 nm. The fluorescence spectra were taken with a protein concentration of 6.5 μM. To the 6.5 μM protein stock solution, different volumes of the buffer were added followed by the requisite volumes of stock additive solutions to obtain the samples of desired additive concentration. Intrinsic fluorescence was measured by exciting the protein solution at 280 and 295 nm and emission spectra were recorded in the range of 445–500 nm.

For extrinsic fluorescence measurements in the ANS binding studies, the excitation was set at 380 nm and the emission spectra were taken in the range of 400–600 nm or at a fixed wavelength of 470 nm.

2.5. CD measurements

CD measurements were carried out with a Jasco spectropolarimeter, model J-720, equipped with a microcomputer. The instrument was calibrated with D-10-camphorsulfonic acid. All the CD measurements were carried out at 25 °C with a thermostatically controlled cell holder attached to a Neslab RTE-110 water bath with an accuracy of ±0.1 °C. Spectra were collected with a scan speed of 20 nm/min and response time of 1 s. Each spectrum was the average of four scans. The far-UV CD spectra were measured at a protein concentration of 6.5 μM at a path length of 1 mm. The secondary structure was estimated from spectra between 200 and 240 nm using K_2d CD secondary structure server, which uses an unsupervised neural network to predict secondary structure [48].

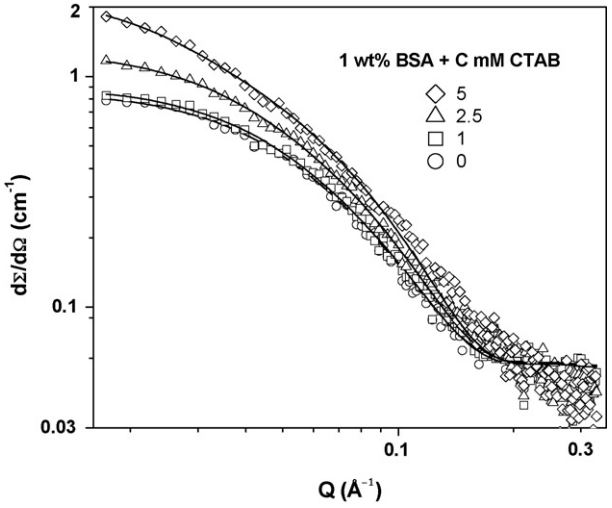

Fig. 1. SANS data of BSA at pH 7, in the presence of 0–5 mM CTAB (temperature 25 °C).

3. Results and discussion

3.1. SANS measurements

SANS data for 1 wt% BSA of varying CTAB concentrations in a buffer solution of pH 7.0 are shown in Figs. 1 and 2. Based on the features of the scattering profiles, the data can be grouped in two different sets (Figs. 1 and 2). The first set (Fig. 1) corresponds to proteins at low surfactant concentrations (0–5 mM) where the scattering data show behavior similar to that of the pure protein solution. In this data set, the overall cross-section increases with increase in surfactant concentration. SANS data in this particular case can be explained in terms of Eq. (1) which considers protein as prolate ellipsoidal in shape. At low surfactant concentrations, the individual surfactant monomers bind to protein and the volume of the scattering particle increases. The features of the scattering profile in the second set (Fig. 2) at higher surfactant concentrations (≥7.5 mM) are significantly different to those of the first data set. One of the interesting features is the linearity of the scattering profiles on log–log scale in the intermediate Q range with the linearity increasing with surfactant concentration. This is an indication of fractal structure by the protein–surfactant complex [8–10]. The build up of scattering cross-section in the higher cut-off of the

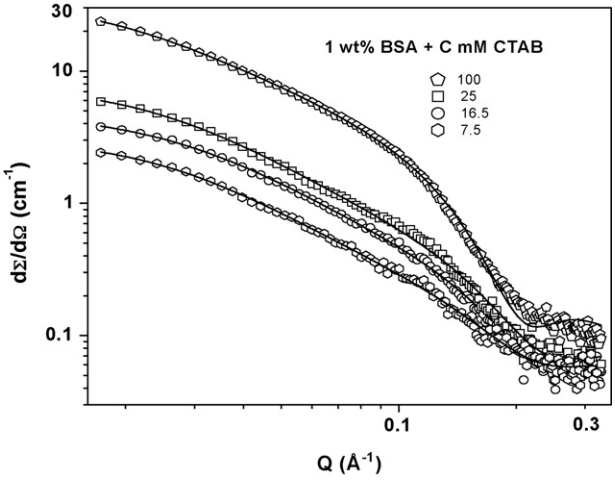

Fig. 2. SANS data of BSA at pH 7, in the presence of 7.5–100 mM CTAB (temperature 25 °C).

Table 1
Fitted parameters of SANS analysis for 1 wt% BSA in the presence of 0–5 mM CTAB.

[CTAB] (mM)	Semi-major (Å)	Semi-minor (Å)
0	70.7 ± 5.1	21.1 ± 0.7
1	71.9 ± 5.2	21.2 ± 0.7
2.5	85.7 ± 6.4	21.1 ± 0.7
5	138.4 ± 10.1	21.0 ± 0.7

linearity of the scattering data suggests the formation of surfactant aggregates and the lower cut-off corresponds to the overall size of the protein–surfactant complex.

The fitted parameters of the SANS data for two sets Figs. 1 and 2 are given in Tables 1 and 2, respectively. It is found that in pure protein solution, the protein macromolecules have a prolate ellipsoidal shape with the semi-major and semi-minor axes as 70.7 and 21.0 Å, respectively. This result is in good agreement to those reported earlier [9,10]. In the first data set, the protein macromolecules maintain their folded structure on addition of surfactant. It is believed that individual surfactant molecules bind to the protein at low surfactant concentration. Table 1 shows changes in the dimensions of the protein on increasing binding of surfactant molecules as a function of surfactant concentration. We observe from the SANS data that, while the semi-major axis becomes double, there is no significant change in the value of semi-minor axis on addition of CTAB in the concentration range 0–5 mM. It is believed that the six protein sub-domains forming BSA remain intact but separate from each other, leading to an elongation of the protein on addition of surfactant. Similar results have also been observed of the complexes of BSA with other surfactants such as sodium dodecyl sulfate [49] and azobenzenetrimethylammonium bromide [50].

Based on the linearity of the scattering data on log–log scale, the second data set has been explained using fractal structure (Eq. (6)) of protein–surfactant complex. The buildup of scattering intensity in the high-Q region of the SANS data suggests that micelle-like clusters are formed along the unfolded polypeptide chain of the protein. The slope of the scattering data on log–log scale gives the value of the fractal dimension D of the complex. The cut-off of the linear range of the data at low and high Q values are respectively, related to the formation of the extent of the complex and the size of the individual micelles in the complex [46]. The fitted parameters of analysis are given in Table 2. It is found that the fractal dimension decreases and shows a relatively same behavior up to 25 mM surfactant concentration with the correlation length also remaining the same. However, at 100 mM concentration there is a significant decrease in fractal dimension corresponding to increase in correlation length. Also, the size of the micelle-like clusters and the number of such clusters does not change till the surfactant concentration of 25 mM, while an increase in the size as well as number is observed at a surfactant concentration of 100 mM. The calculated aggregation number of micelle-like clusters (n) in the complex increases from 25 to 97 on increasing surfactant concentration from 7.5 to 100 mM. Some experiments were also performed with TTAB. Similar to CTAB, TTAB (Fig. 3) brings about an increase in the size of the protein along the semi-major axis at low surfactant concentrations and forms a fractal structure at high concentrations. At 5 mM [TTAB], the semi-major axis of BSA increases to 94 Å while

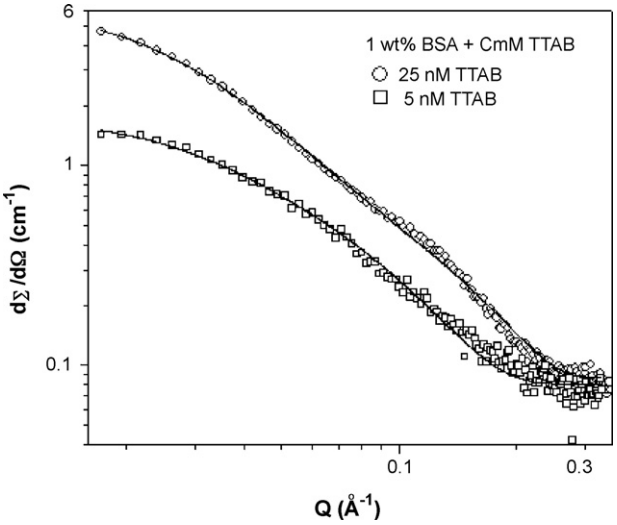

Fig. 3. SANS data of BSA at pH 7, in the presence of 5 mM and 25 mM TTAB (temperature 25 °C).

the formation of a fractal structure with a fractal dimension equal to 2.26 is observed at 25 mM.

3.2. Intrinsic fluorescence

Variations in the fluorescence intensity and the wavelength of emission maximum (λ_{max}), parameters sensitive to protein conformation can be effectively used to probe protein folding/unfolding. The fluorescence of proteins originates entirely from the tyrosine and tryptophan residues. Two tryptophan residues, Trp-134 in the eighth helix of D12-R144 in domain I, and Trp-213 in the second helix of E206-F221 in domain II are present in a BSA molecule [51]. The variations in the fluorescence spectra obtained by exciting the protein at 295 nm are attributed to the presence of tryptophan residues while the changes at 280 nm are mainly associated with tyrosine residues.

Figs. 4 and 5, respectively, illustrate the emission spectra of native BSA and BSA mixed with CTAB at the excitation wavelengths of 295 and 280 nm. It is observed that that the intrinsic fluorescence intensities increase coupled by a decrease in λ_{max} or blue shift with the increasing surfactant concentration, indicating unfolding of the protein. These changes are significant at the excitation wavelength of 295 nm (Fig. 4) compared to 280 nm (Fig. 5) suggesting that tryptophan is the main contributor of BSA fluorescence. The native protein (curve 1, Fig. 5) with the λ_{max} at 342 nm also indicates that BSA is dominated by tryptophan emission [52]. It is observed that the fluorescence intensity at 330 nm remains almost unchanged at the surfactant concentration of 1 mM (curve 2) with a 2 nm blue shift (λ_{max} = 344 nm) suggesting native-like behavior of BSA. The fluorescence spectra observed at a surfactant concentration of 2.5 mM (curve 3) and 5 mM (curve 4) do not show any significant change. The fluorescence changes markedly with some rise in fluorescence intensity and a blue shift of 9 nm (λ_{max} = 333 nm) at the CTAB concentration of 7.5 mM (curve 5) suggesting unfolding of the protein. The unfolding continues till 16.5 mM CTAB (curve 6)

Table 2
Fitted parameters of SANS analysis for 1 wt% BSA in the presence of 7.5–100 mM CTAB.

[CTAB] (mM)	Fractal dimension	Micellar radius (Å)	Zhi (Å)	Number of such micelles in the complex	Aggregation number, n
7.5	2.23 ± 0.15	17 ± 0.6	34.3 ± 1.5	1.8	25
16.5	2.16 ± 0.14	17 ± 0.6	32.0 ± 1.4	1.9	53
25	2.23 ± 0.15	17 ± 0.6	37.4 ± 1.8	2.3	66
100	1.74 ± 0.04	20.5 ± 0.7	62 ± 4.2	6.2	97

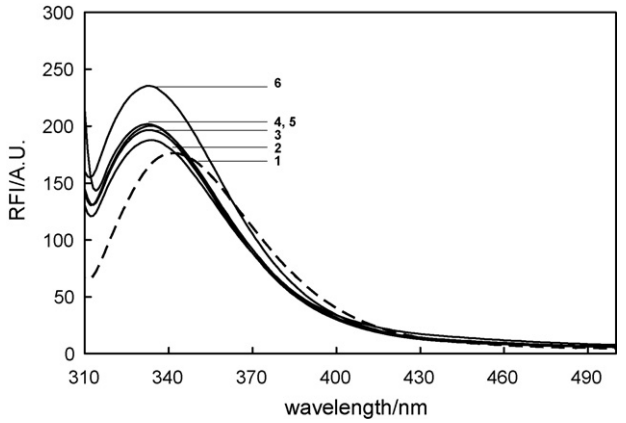

Fig. 4. Fluorescence spectra of the BSA at pH 7 in the native state (1) and in the presence of 1 mM (2), 2.5 mM (3), 5 mM (4), 7.5 mM (5) and 16.5 mM (6) CTAB when excited at 295 nm (temperature 25 °C).

as is indicated by a considerable increase in fluorescence intensity and a blue shift of 5 nm (λ_{max} = 328 nm). The significant increase in the fluorescence intensity is associated to the fact that at low surfactant concentration only the helix of Trp-134 is active to interact with the surfactant, while at high concentration, Trp-213 is also exposed to the surface of BSA (due to unfolding). Besides unfolding, the decrease in λ_{max} at higher surfactant concentration indicates the formation of micelles on the protein backbone leading to a hydrophobic environment and a consequent blue shift. These results, suggesting native-like behavior of the protein at very low surfactant concentration, unfolding (as the concentration of the surfactant increases), and creation of a hydrophobic environment due to micelle formation along the polypeptide chain at still higher surfactant concentrations, are in perfect cognizance with the SANS measurements.

3.3. Extrinsic fluorescence

1-Anilino-8-naphthalenesulfonate (ANS) is a widely used fluorescent probe known to bind to the hydrophobic patches of the protein [53]. There are two different apparent ranges over which ANS binds to the proteins like serum albumins [54]. One of these is a broad range involving as many as 100 binding sites at pH's below 5, where most of the bound ANS is not fluorescent. In a much narrower range of binding, where ANS is assumed to act as a hydrophobic probe, ANS may become fluorescent. Five hydrophobic sites have been detected on native serum albumins in the pH range 5–7 [55,56]. The fluorescence exhibited by the native HSA at pH 7 is associated with the presence of these hydrophobic patches and the variation of the fluorescence intensity can be effectively used to monitor the accessibility of the hydrophobic patches. Generally, increase in ANS protein binding indicates opening of hydrophobic sites and thus unfolding of protein and vice versa.

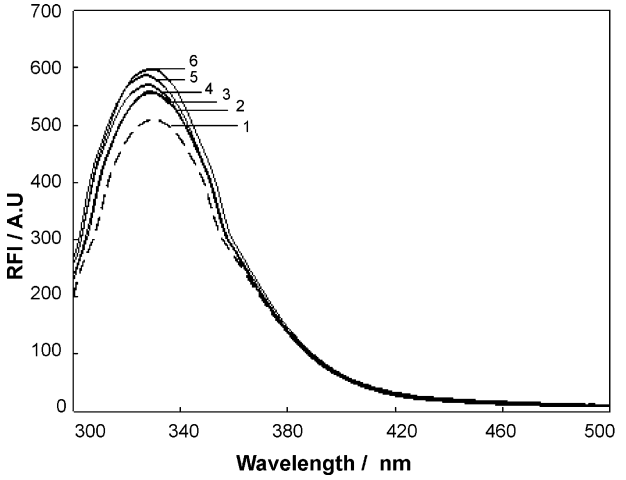

Fig. 5. Fluorescence spectra of the BSA at pH 7 in the native state (1) and in the presence of 1 mM (2), 2.5 mM (3), 5 mM (4), 7.5 mM (5) and 16.5 mM (6) CTAB when excited at 280 nm (temperature 25 °C).

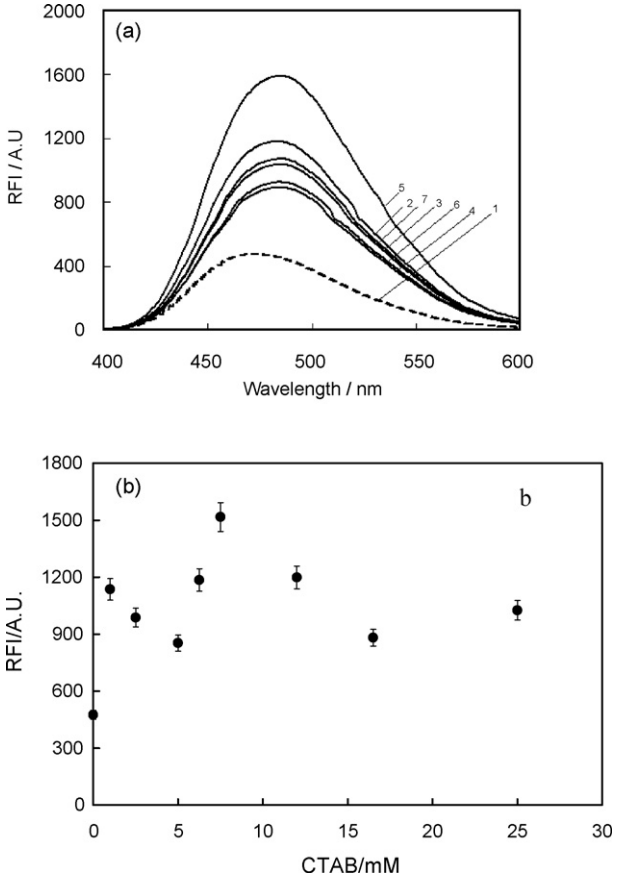

Fig. 6. (a) Fluorescence spectra of ANS bound BSA at pH 7 in the presence of varying amounts of CTAB when excited at 380 nm [CTAB] = 0 mM (1), 1 mM (2), 2.5 mM (3), 5 mM (4), 7.5 mM (5), 16.5 mM (6) and 25 mM (7) CTAB (temperature 25 °C). (b) RFI of ANS bound BSA (6.5 μM) at pH 7 in the presence of CTAB on the basis of fluorescence intensity at 470 nm by exciting at 380 nm.

Fig. 6a illustrates the Fluorescence spectra of BSA in the native state and ANS bound BSA at pH 7 in the presence of varying amounts of CTAB when excited at 380 nm. Changes in the relative fluorescence intensities (RFI) of ANS bound BSA at pH 7 in the presence of CTAB on the basis of fluorescence intensity at 470 nm are plotted in Fig. 6b. The initial increase in the ANS binding depicted by curve 2 (1 mM CTAB) is due to the co-binding of the surfactant and the probe molecules near the hydrophobic regions of the protein. The decrease observed afterwards, at 2.5 mM CTAB (curve 3) and 5 mM CTAB (curve 4), indicates the release of some of the probe molecules into a more hydrophilic phase because of the competition for binding with the surfactant. Beyond the minimum, the fluorescence intensity rises and the probe again reports an increase in the hydrophobicity at 7.5 mM CTAB (curve 5). The surfactant at such concentrations binds to the protein and unfolds it, exposing more and more hydrophobic patches and consequently increasing the ANS binding. The increase in the ANS binding in this region is due to the binding of the probe and the surfactant molecules to the hydrophobic regions made available by the protein unfold-

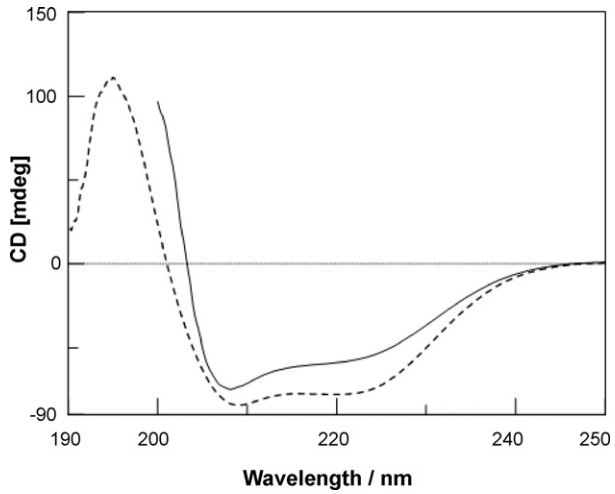

Fig. 7. Far UV-CD spectra of BSA in the absence (- - -) and presence (—) of 1 mM CTAB.

ing. The decrease in ANS binding observed at CTAB concentration of 16.5 mM (curve 6) is associated with the displacement of the protein-bound ANS by the CTAB micelles and the consequent expulsion of the probe molecules into the aqueous phase till the ANS binding assumes some constant minimum value at a CTAB concentration of 25 mM (curve 7). The results obtained from the extrinsic fluorescence studies corroborate well with the intrinsic fluorescence as well as SANS measurements.

3.4. Far-UV CD

Alterations of ellipticity at 222 nm ($-MRE_{222}$) are useful probe for visualizing varying α-helical contents [57]. Circular dichroism (CD) measurements were, therefore, performed to monitor the changes of the secondary structure generated by the interaction of BSA with CTAB. The absorbance of the samples is conveniently measured by the trace of the high-tension voltage. The high-tension voltage was found to remain within the permissible limits for native BSA and BSA mixed with 1 mM CTAB only. The higher CTAB concentrations could not be measured due to very high dynode voltage.

Fig. 7 shows the far-UV CD spectra of BSA in the native state and in the presence of 1 mM CTAB. The CD spectra of BSA mixed with 1 mM CTAB could not be monitored beyond 200 nm because of noise detected below this wavelength. The spectrum of untreated BSA at pH 7 shows negative minima nearly at 208 and 222 nm, characteristic of α-helical structure [58]. The untreated BSA contained about 65% α-helical structure as estimated by K_2d [48]. This is in good agreement with the literature value [35]. BSA shows a decrease in CD values at a 1 mM concentration of CTAB, as shown in the Fig. 7, indicating a decrease in α-helical content. The helical content, as determined by K_2d (Table 3), is found to decrease from 65% for native BSA to 57% in presence of 1 mM CTAB. This small decrease in the α-helical content does not affect the overall protein conformation much and the protein thus retains a native like structure as demonstrated by SANS and fluorescence measurements.

Table 3
Analysis of possible secondary structure contents on the basis of far UV-CD, calculated by K_2d.

[CTAB] (mM)	Alpha helicity (%)	Beta sheet (%)	Random coil (%)
0	65	5	29
1	57	10	34

4. Conclusion

SANS measurements were carried out to investigate the changes in the structure of protein on the addition of varying concentration of surfactants CTAB and TTAB. The binding of ionic surfactants to protein is found to disrupt the native structure of the protein. At low surfactant concentrations, an increase in the dimension of the ellipsoidal protein is observed. As indicated by the data, the semi-major axis is found to remain more or less constant and the changes occur mostly along the semi-major axis. A fractal structure at higher concentrations suggests the formation of micelle-like clusters in the protein–surfactant complex. The low surfactant concentration region is related to the binding that occurs at specific sites through electrostatic interactions while the higher surfactant concentration is associated with the cooperative surfactant interaction resulting in the unfolding of the protein. The conformational changes observed in the protein by fluorescence spectroscopy suggesting native-like behavior at low surfactant concentration and unfolding at high concentration are found to be in tune with the results obtained from SANS measurements. Though limited, the CD data do indicate a small decrease in the α-helical content at low surfactant concentration and hence confirm the above results.

References

[1] H. Guo, N.M. Zhao, S.H. Chen, J. Teixeira, Biopolymers 29 (1990) 335.
[2] C. Tanford, The Hydrophobic Effect: Formation of Micelles and Biological Membranes, 2nd ed., Wiley Interscience, New York, 1980.
[3] M.L. Anson, Science 90 (1939) 256.
[4] J.C. Rochet, P.T. Lansbury Jr., Curr. Opin. Struct. Biol 10 (2000) 60.
[5] A. Helenius, K. Simons, Biochim. Biophys. Acta 415 (1975) 29.
[6] O.T. Jones, J.P. Earnest, M.E. McNamee, in: J.B.C. Findley, W.H. Evans (Eds.), Biological Membranes, IRL Press, Oxford, 1987.
[7] D. Kelley, D.J. McClements, Food Hydrocolloids 17 (2003) 73.
[8] J. Chamani, J. Colloid Interface Sci. 299 (2006) 636.
[9] C. Honda, H. Kamizono, K. Matsumoto, K. Endo, J. Colloid Interface Sci. 278 (2004) 310.
[10] S.F. Santos, D. Zenette, H. Fischer, R. Itri, J. Colloid Interface Sci. 262 (2003) 400.
[11] A. Wangsakan, P. Chinachoti, D.J. McClements, Langmuir 20 (2004) 3913.
[12] A.V. Few, R.H. Ottewill, H.C. Parreira, Biochim. Biophys. Acta 18 (1955) 136.
[13] Y. Nozaki, J.A. Reynolds, C. Tanford, J. Biol. Chem. 249 (1974) 4452.
[14] S. Ray, A. Chakrabarti, Cell Motil. Cytoskeleton 54 (2003) 16.
[15] M.A. McCoy, D.F. Wyss, J. Am. Chem. Soc. 124 (2002) 2104.
[16] E.D. Goddard, K.P. Ananthapadmanabhan, Interaction of Surfactants with Polymers and Proteins, CRC Press, London, 1993.
[17] S. Deep, J.C. Ahluwalia, Phys. Chem. Chem. Phys. 3 (2001) 4583.
[18] Q. Xu, T.A. Keiderling, Prot. Sci. 13 (2004) 2949.
[19] A. Stenstam, D. Topgaard, H. Wennerström, J. Phys. Chem. 107 (2003) 7987.
[20] M.N. Jones, H.A. Skinner, E. Tipping, Biochem. J. 147 (1975) 229.
[21] J.C. Gimel, W. Brown, J. Chem. Phys. 104 (1996) 8112.
[22] S.H. Chen, J. Teixeira, Phys. Rev. Lett. 57 (1986) 2583.
[23] X.H. Guo, S.H. Chen, Phys. Rev. Lett. 64 (1990) 1979.
[24] E. Seth, V.K. Aswal, J. Macro. Sci.: Phys. B 42 (2003) 85.
[25] C.T. Lee Jr., K.A. Smith, T.A. Hatton, Biochemistry 44 (2005) 524.
[26] E.L. Galemo, R. Itri, A. Alonso, J.V.D. Silva, M. Tabak, J. Colloid Interface Sci. 277 (2004) 471.
[27] B. Schweitzer, D. Zanette, R. Itri, J. Colloid Interface Sci. 277 (2004) 285.
[28] M.N. Jones, D. Chappman, Micelles, Monolayers and Biomembranes, Wiley-Riss, New York, 1995.
[29] T. Peters Jr., All about Albumins: Biochemistry, Genetics and Medical Applications, Academic Press, San Diego, 1996.
[30] D. Carter, B. Chang, J.X. Ho, K. Keeling, Z. Krishnaswamy, Eur. J. Biochem. 226 (1994) 1049.
[31] J.R. Brown, P. Shockley, Lipid–Protein Interactions, vol. 1, Wiley, New York, 1982.
[32] X. Min He, D. Carter, Nature 358 (1992) 209.
[33] D. Carter, J.X. Ho, Advances in Protein Chemistry, vol. 45, Academic Press, New York, 1994.
[34] S. Curry, H. Mandelkow, P. Brick, N. Franks, Nat. Struct. Biol. 5 (1998) 827.
[35] R. Narazaki, T. Murayama, M. Otagiri, Biochim. Biophys. Acta 1338 (1997) 275.
[36] N. Chadborn, J. Bryant, A.J. Bain, P. O'Shea, Biophys. J. 76 (1999) 2198.
[37] J.A. Reynolds, S. Herbert, H. Polet, J. Steinhardt, Biochemistry 6 (1967) 937.
[38] T. Kosa, T. Maruyama, M. Otagiri, Pharm. Res. 14 (1997) 1607.
[39] F. Moreno, M. Cortijo, J.G. Jimenez, Photochem. Photobiol. 69 (1999) 8.
[40] M.E. Holt, M.E. Ryall, A.K. Campbell, Br. J. Exp. Pathol. 65 (1984) 231.
[41] D. Barnes, G. Sato, Anal. Biochem. 102 (1980) 255.
[42] S.M. Callister, K.L. Case, W.A. Agger, R.F. Schell, R.C. Johnson, J.L. Ellingson, J. Clin. Microbiol. 28 (1990) 363.
[43] P.S. Goyal, V.K. Aswal, Curr. Sci. 80 (2001) 972.

[44] G.D. Wignall, F.S. Bates, J. Appl. Cryst. 20 (1987) 28.
[45] J.B. Hayter, J. Penfold, Colloid Polym. Sci. 261 (1983) 1022.
[46] J. Teixeira, J. Appl. Cryst. 21 (1988) 781.
[47] P.R. Bevington, Data Reduction and Error Analysis for Physical Sciences, McGraw-Hill, New York, 1969.
[48] M.A. Adrade, P. Chacon, J.J. Merelo, F. Moran, Protein Eng. 6 (1993) 383.
[49] S. Chodankar, V.K. Aswal, J. Kohlbrecher, R. Vavrin, A.G. Wagh, J. Phys.: Condens. Matter. 19 (2007) 326102.
[50] T.C. Lee, K.A. Smith, A.T. Hatton, Biochemistry 44 (2005) 524.
[51] A.D. McLachlan, J.E. Walker, J. Mol. Biol. 112 (1977) 543.
[52] S. Era, K.B. Itoh, M. Sogami, K. Kuwata, T. Iwama, H. Yamada, H. Watari, Int. J. Pept. Protein Res. 35 (1990) 1.
[53] L. Stryer, J. Mol. Biol. 3 (1965) 482.
[54] D. Matulis, R. Lovrien, Biophys. J. 74 (1998) 422.
[55] J. Slavik, Biochem. Biophys. Acta 694 (1982) 1.
[56] E. Daniel, G. Weber, Biochemistry 5 (1966) 1893.
[57] R.F. Chen, Arch. Biochim. Biophys. 160 (1974) 106.
[58] J. Carbin, N. Methlot, H.H. Wang, J.E. Baenziger, P. Blanton, J. Biol. Chem. 273 (1998) 771.